Received: 19 May 2022 | Revised: 5 August 2022 | Accepted: 12 September 2022

DOI: 10.1002/mawe.202200119

ARTICLE

WILEY VCH

Effects of process parameters on fatigue behavior and surface integrity of tool steel produced by electrical discharge turning

Auswirkungen von Prozessparametern auf das Ermüdungsverhalten und die Oberflächenintegrität von durch Funkenerosionsdrehen hergestelltem Werkzeugstahl

R. Çakıroğlu[1] | **M. Günay**[2]

[1]Gazi University, Vocational School of Technical Sciences, Ankara, Turkey

[2]Karabük University, Engineering Faculty, Karabük, Turkey

Correspondence
M. Günay, Karabük University, Engineering Faculty, 78050 Karabük, Turkey.
Email: mgunay@karabuk.edu.tr

Abstract

Electrical discharge machining is used in the production of countless parts with complex geometries and micro dimensions, from many elements of industrial molds to parts of motors and pumps. Also, most of these parts are cylindrical and it is always more meaningful to study their rotational fatigue behavior to predict their response during their operation. This study concentrated on the impacts of machining parameters on the surface quality and fatigue behavior of tool steel shaped by electrical discharge turning. The results based on Taguchi methodology have shown that discharge current affects R_a and R_z more, and pulse duration more affects the mean spacing of profile irregularities, S_m. As a result of the heat affected depth in the machined region, which changes in proportional with the processing parameters, the microhardness decreased from the sample surface to the core. The maximum hardness was measured at current of 12 A, pulse duration of 3 μs and pulse interval of 7 μs. According to the fatigue tests, it was found that the fatigue life decreased with the increase in R_z and S_m values. Moreover, high microhardness and thick recast layer reduced the fatigue strength of the samples with relatively smooth surface topography.

KEYWORDS
electrical discharge machining (EDM), fatigue behavior, microhardness, surface topography, tool steel

SCHLÜSSELWÖRTER
Ermüdungsverhalten, Funkenerodieren, Mikrohärte, Oberflächentopographie, Werkzeugstahl

© 2023 Wiley-VCH GmbH.

15214052, 2023, 1, Downloaded from https://onlinelibrary.wiley.com/doi/10.1002/mawe.202200119 by Gazi University, Wiley Online Library on [28/01/2023]. See the Terms and Conditions (https://onlinelibrary.wiley.com/terms-and-conditions) on Wiley Online Library for rules of use; OA articles are governed by the applicable Creative Commons License

1 | INTRODUCTION

Electrical discharge machining (EDM) is commonly used in the manufacture of mechatronic systems for instance injection molding, powder metallurgy and forging dies, punches, pump parts, motors, robots, power reactors and biomedical device parts, and especially in the creation of machine parts with complex geometry and micro-dimensional holes that are difficult to produce with traditional machining methods. On the other hand, it is impossible to produce a cylindrical part by die-sinking electrical discharge machining. Therefore, numerous electrical discharge machining practices in accordance with the basic principles of electrical discharge machining are implemented in the manufacturing industry, including very specific styles such as drilling, grinding, turning, honing, and wire electrical discharge machining [1]. It has been confirmed in research that the mentioned electrical discharge machining techniques can be applied in the machining of micro-sized cylindrical parts and grooves with desired quality [2].

Fatigue life of machined parts varies according to the material structure, machining process and parameters. Therefore, surface integrity of machined parts is fundamental to determine the functional characteristics like corrosion strength, fatigue and tribological characteristics. Surface integrity includes surface changes such as surface topography, phase alterations, microhardness, cracks, and residual stress [3, 4]. Roughness is an important surface topography gauge that affects fatigue life by creating an indentation effect. In each of the traditional or non-traditional machining techniques, dissimilar roughness patterns occur depending on the cutting conditions. Therefore, although it has been known for many years that surface roughness is an important factor affecting fatigue behavior, the role played by machining processes in this area still represents an active research topic [5]. The surface pattern in electrical discharge machining has a crater-like form that is completely altered from those obtained in other processing methods. In addition, high temperatures in non-traditional machining can influence surface integrity indicators such as recast layer, microcracks, residual stresses, and also as well as microstructural and hardness changes, albeit very shallow [6, 7]. Recast layers exhibit improved stiffness matched to bulk material with a state of residual stress in the form of tension and often contain microcracks. All these can reduce the fatigue life of machined components [8, 9]. Recently, it has been emphasized that material removal rate and surface integrity can be improved with ultrasonic vibration electrical discharge applications, but the need for optimization of ultrasonic vibration power is emphasized [10, 11]. Electrical discharge machining inherently has many complex and random metal removal processes. Therefore, it is enormous problem to set the best machining parameters for high material removal rate and ideal surface quality, which means increased machining cost. Because the machinability indicators such as material removal rate, surface topography, electrode wear ratio and dimensional precision are naturally inconsistent [12, 13]. Particularly in the electrical discharge turning, it is very difficult to regulate a single best set of machining parameters, as the parameters influence machinability indicators in many ways. In order to reach the mentioned solution, it should be done with multiple optimization methods for example the gray relational analysis approach [14, 15].

There are many studies on the fatigue life of samples produced from various materials using electrical discharge machining technologies. In some of these studies conducted in recent years, the effects of wire electrical discharge machining parameters on surface integrity and fatigue behavior for Inconel 718, Ti-6Al-4 V alloy and Si3 N4-TiN material [16–18]. In another study, Inconel 718 parts produced under optimum machining conditions with electrical discharge machining turning were compared with conventional finish turning in terms of machining time and fatigue life. In finish turning, the machining time was only 7% shorter than the proposed hybrid electrical discharge machining approach, while the fatigue life was approximately 43% lower [19]. Or else the effects of process parameters on fatigue life of the samples in the electrical discharge machining and grinding of D2 tool steel, the electrical discharge machining and milling of austenitic stainless steel and the electrical discharge machining of annealed tool steel were investigated [20–22]. In the studies, it is also seen that the samples are according to axial loading or bending fatigue test. However, since most of the machine elements have cylindrical or complex geometries, it is considered more meaningful to examine the rotating bending fatigue test in order to better predict the dynamical behavior of these parts under operating conditions. At the same time, tool steels are used in tooling and the production of many die and mold parts [23]. Moreover, it is understood from the literature that there are limited studies on the fatigue relationship and electrical discharge machining of these materials. So, fatigue behavior of cylindrical samples produced from AISI L2 tool steel by electrical discharge turning (EDT) was investigated. For this purpose, the interactions between the most effective parameters on the part quality in the electrical discharge turning (discharge current, pulse duration and interval) and surface quality, microhardness and fatigue life were analyzed.

15214052, 2023, 1, Downloaded from https://onlinelibrary.wiley.com/doi/10.1002/mawe.202200119 by Gazi University, Wiley Online Library on [28/01/2023]. See the Terms and Conditions (https://onlinelibrary.wiley.com/terms-and-conditions) on Wiley Online Library for rules of use; OA articles are governed by the applicable Creative Commons License

2 | EXPERIMENTAL SETUP AND MEASUREMENTS

The goal of this work is to investigate the effects of machining parameters on surface integrity and fatigue behavior of parts formed by electrical discharge machining. In this context, examinations were made on cylindrical fatigue test samples in order to predict the behavior of the part produced with electrical discharge machining in different service conditions. Therefore, fatigue samples were produced with die-sinking electrical discharge turning in accordance with ASTM E466. For this purpose, a turning system was designed and fixed to the work table of the electrical discharge machining machine. Details about the rotation mechanism and the working principle of the system in the electrical discharge machining machine are given in our previous study [24]. Die-sinking electrical discharge turning tests were conducted by an electrical discharge machining machine with Furkan M25 model pulse generator. In electrical discharge turning processes, kerosene with 2 bar washing pressure was used as dielectric environment. The process was started by connecting the electrode to the negative pole and the workpiece to the positive pole.

A tool steel (115CrV3), is frequently used in the manufacture of various die set parts and cold forming tools, was selected as the material to be machined. In order to speed up the electrical discharge machining process and thus reduce the processing time and costs, the samples for electrical discharge turning were first brought to a certain size on the computer numerical control (CNC) machine. Then, the electrode was designed and prepared by wire electrical discharge machining from 99.5% pure copper materials to produce the fatigue samples based on ASTM E466. As stated in our previous study, the optimum rotation speed for electrical discharge turning was determined as 1 Hz as a result of preliminary tests [24]. The machining parameters were chosen based on the range of values recommended by the machine builder for the die-sinking electrical discharge machining. Die-sinking electrical discharge turning processes were done by using the L_9 experiment design to save time and cost, Table 1.

After the electrical discharge turning experiments, the measurements of the surface roughness criteria were made as a first step. The average surface roughness (R_a), maximum roughness depth (R_z) and mean spacing of profile irregularities (S_m) values were measured using a Form Talysurf PGI profilometer with a cutting length of 0.8 mm and a sampling length of 5.6 mm. The above-mentioned surface roughness criteria (R_a, R_z and S_m) were measured three times right in the middle of the machined samples for each machining condition. In addition, measurements were made immediately after the experiments to prevent oxidation in the samples. The results were evaluated by taking the average of the roughness measurements made after 3 repeated experiments. In the second step, the processed samples were mounted from the cylindrical part in order to make microhardness measurements and polishing was carried out using 400, 800, 1200 and 2000 sandpapers. Microhardness was measured using the Vickers hardness measurement method. These measurements were made by applying a load of 0.1 kg per unit area on a Shimadzu brand hardness measuring device. Microhardness measurements were made from seven different points from the cylindrical outer surface to the center with 20 μm spacing for each of the test samples. In final stage, 15 test specimens were prepared with electrical discharge turning for each machining condition in order to generate Wöhler fatigue diagrams based on ASTM E-466 standard. A rotational bending fatigue device was used in the fatigue tests. The experimental setup and measurement procedures are shown in as a flow chart, Figure 1.

TABLE 1 Taguchi L_9 experimental design.

Exp. no	Discharge current (*Ip*)	Pulse duration (*Ton*)	Pulse interval (*Toff*)
1	3	3	5
2	3	6	6
3	3	8	7
4	6	3	6
5	6	6	7
6	6	8	5
7	12	3	7
8	12	6	5
9	12	8	6

3 | RESULTS AND ASSESSMENT

3.1 | Surface quality

An increase in the discharge current means an increment in the thermal energy transferred to the workpiece, thus removing more chips from the workpiece. This process creates deeper and wider craters on the machined surface, resulting in an increase in surface roughness [25, 26]. R_a value increased with the rise of discharge current and pulse duration in the die-sinking electrical discharge turning method, as in die-sinking

15214052, 2023, 1, Downloaded from https://onlinelibrary.wiley.com/doi/10.1002/mawe.202200119 by Gazi University, Wiley Online Library on [28/01/2023]. See the Terms and Conditions (https://onlinelibrary.wiley.com/terms-and-conditions) on Wiley Online Library for rules of use; OA articles are governed by the applicable Creative Commons License

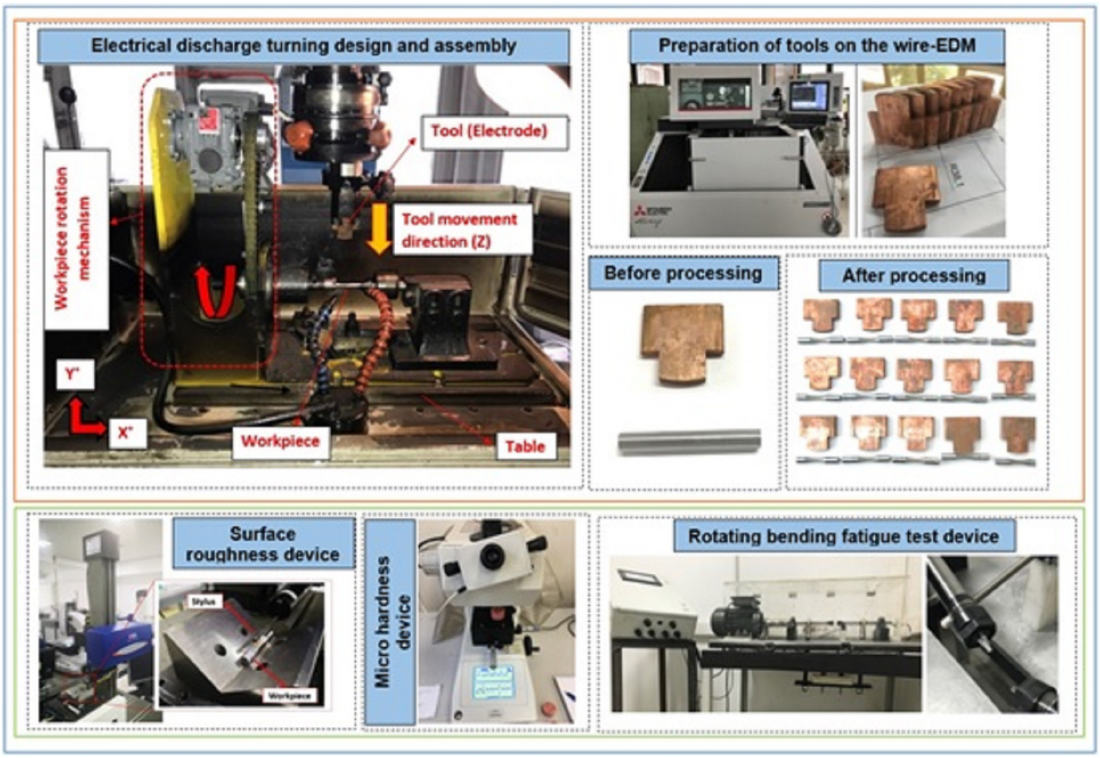

FIGURE 1 Flow diagram for experiments and measurements.

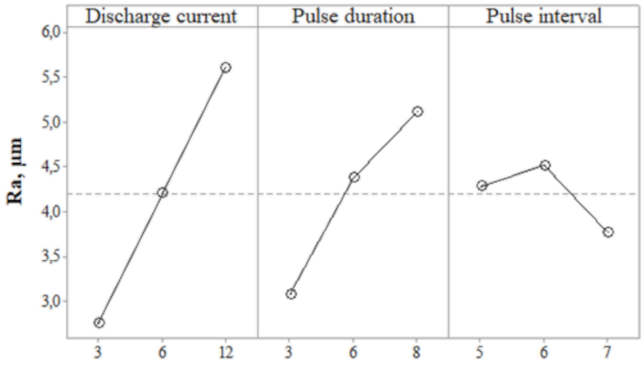

FIGURE 2 R_a variation according to process parameters.

electrical discharge machining, Figure 2. The macro surface images of machined parts shows that the R_a values increase linearly as the pulse duration rises, Figure 3. As a result, the increase in thermal deformation caused by the increase in pulse duration caused an increase in R_a values similar to the current effect. On the other hand, the change in Ra values did not show a parallel trend with the increase in the pulse interval. This is thought to be due to the Taguchi experimental design, Figure 1. If this table is examined, the surface roughness first increased and then decreased due to the random distribution of pulse interval levels. In addition, the falling time of the spark varied for each discharge current value as the pulse interval increased. With the increase in the discharge period, the workpiece was exposed to temperature for a longer time and the amount of melting in the material increased gradually. In this case, as stated in some studies multidirectional irregular and randomly distributed deeper craters were formed on the machined surface, resulting in increased surface roughness [4, 8, 24]. When the surface morphology formed in experiment 3 is carefully examined, it can be seen that a crater formation has occurred, which supports the aforementioned result, Figure 3. Besides, despite the increase in discharge current, as in experiment 7, as a result of the cooling in the machining area with the increase of the pulse interval, the material removal decreased and shallower craters were formed on the workpiece surface [11, 27]. The lowest R_a value was obtained as 2.267 µm at discharge current of 3 A, pulse duration of 3 µs and pulse interval of 5 µs.

While R_z increased proportionally as the discharge current increased, it first showed a tendency to increase and then decrease with the rise of the pulse duration and interval, Figure 4. The highest R_z value was obtained as 36.012 µm at 12 A, pulse duration of 8 µs and pulse interval of 6 µs, the lowest R_z value was 14.039 µm at 3 A, pulse duration of 3 µs and pulse interval of 5 µs. As well, when the change of R_z according to the discharge current is evaluated, the greatest change with the increase of the pulse duration is obtained as 41.1% at 12 A. For 3 A and 6 A discharge currents, the proportion of change

15214052, 2023, 1, Downloaded from https://onlinelibrary.wiley.com/doi/10.1002/mawe.202200119 by Gazi University, Wiley Online Library on [28/01/2023]. See the Terms and Conditions (https://onlinelibrary.wiley.com/terms-and-conditions) on Wiley Online Library for rules of use; OA articles are governed by the applicable Creative Commons License

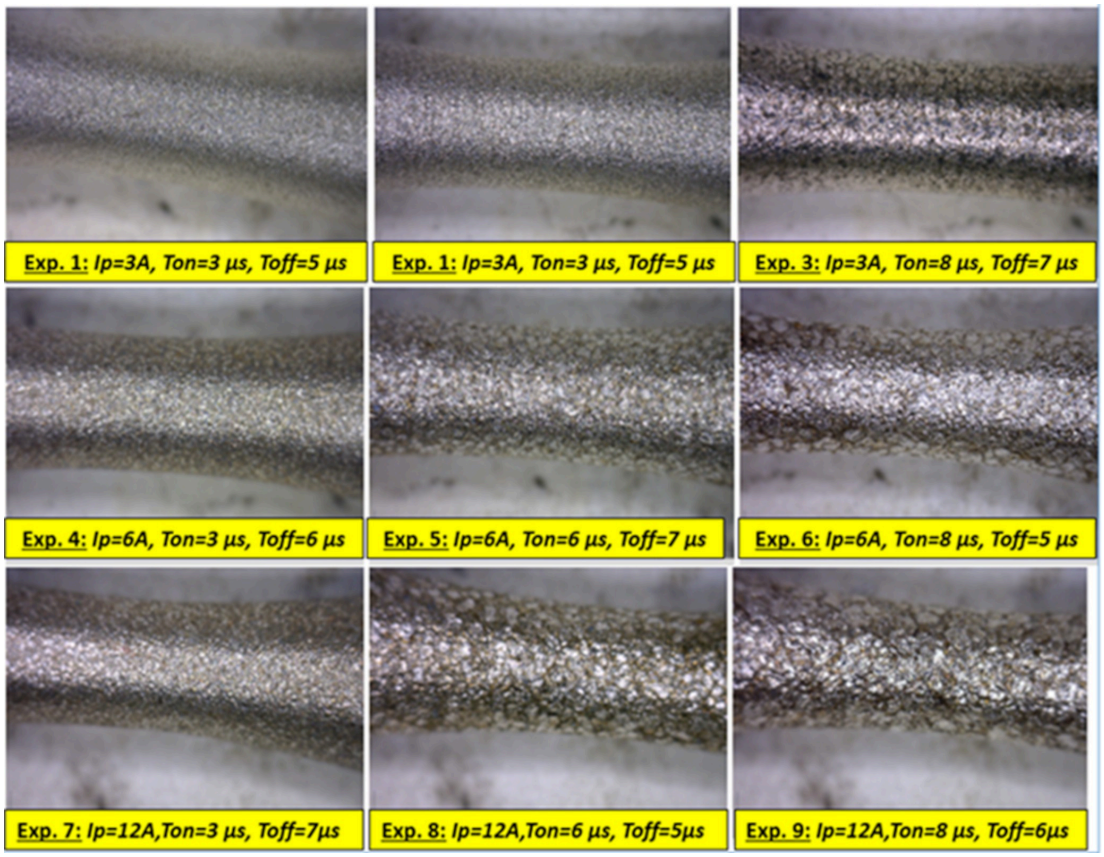

FIGURE 3 Surface images of electrical discharge turning applied samples (50×).

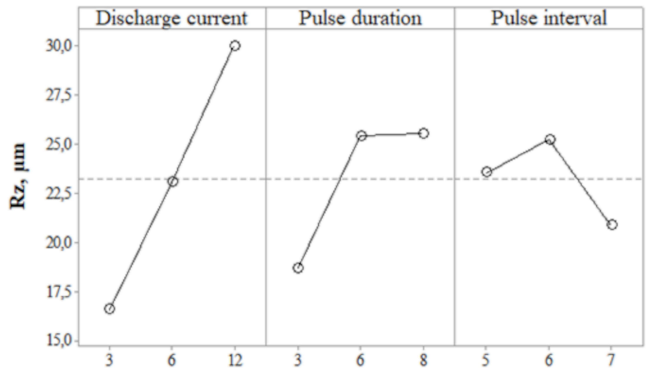

FIGURE 4 R_z variation according to process parameters.

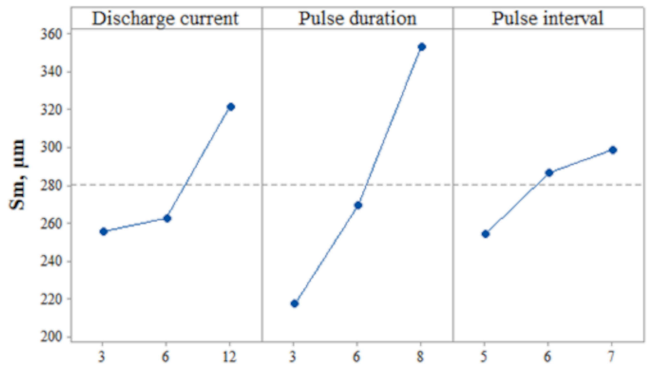

FIGURE 5 Variation of S_m according to process parameters.

of R_z value was calculated as 16.8% and 15.01% on average, respectively. This variation in the R_z value indicates that more thermal deformation occurs on the workpiece surface as a result of the increase in the sparks number with the increasing discharge current. At the same time, longer-term melting and evaporation occur on the workpiece surface owing to the increased discharge energy with the increasing pulse duration [28, 29]. Thus, a surface morphology with deeper craters is formed and this means an increase in roughness values. In the aforementioned experiment, maximizing the pulse interval resulted in a reduction in R_z, at the same time, pulse duration is small here.

Another criterion taken into account in terms of surface topography, S_m, which is also used in the calculation of theoretical fatigue life, is the average of the spaces between the peaks in the roughness profile [30]. The variation of S_m according to the processing parameters is given as graphically, Figure 5. The highest S_m value was measured as 398.187 µm at 12 A, pulse duration of 8 µs and pulse interval of 6 µs, the lowest S_m value was measured as 164.486 µm 3 A, pulse duration of 3 µs

15214052, 2023, 1, Downloaded from https://onlinelibrary.wiley.com/doi/10.1002/mawe.202200119 by Gazi University, Wiley Online Library on [28/01/2023]. See the Terms and Conditions (https://onlinelibrary.wiley.com/terms-and-conditions) on Wiley Online Library for rules of use; OA articles are governed by the applicable Creative Commons License

and pulse interval of 5 μs. When the S_m results were evaluated, the increase in S_m reached to the highest value (53.76%) with the increase of the pulse duration in the experiments at 3 A. The proportion of change of S_m value was determined as 29.5% and 31.5% at 6 A and 12 A values, respectively. Based on these results, it can be said that the most effective parameter is the pulse duration for S_m. It is understood that a surface morphology with deeper and wider craters than the workpiece surface is formed due to the formation of high energy sparks depending on the increase in discharge current and pulse duration. This is in line with the physical logic of die-sinking electrical discharge machining, and similar results have been obtained in different electrical discharge machining applications [26, 31].

3.2 | Microhardness

Microhardness measurements have been performed to characterize the mechanical properties of machined subsurface at the end of the electrical discharge turning. These measurements were made from 7 different points with 20 μm intervals from the surface of the workpiece to the center in order to examine the microhardness change in the fatigue samples. The microhardness results according to the machining parameters are shown as graphically, Figure 6. When this figure is carefully examined, it is seen that the microhardness values decrease from the machined surface to the material core and the hardness of the material reaches its pre-electrical discharge machining value (367 HV). A similar trend was seen in all machining conditions and the highest microhardness was measured from the regions closest to the machined surface. This result is a proof that the mechanical properties and hardness change significantly due to the subsurface formations such as recast layer, heat affected zone that develop due to high temperature gradients in the electrical discharge turning process [32, 33]. In experiments with high discharge current or medium discharge current-high pulse duration, it was determined that the microhardness values were also high. The highest hardness was measured from the 7th test sample as 1376 HV at a distance of 20 μm from the machined surface. The lowest microhardness at the same distance value was obtained as 1150 HV in the 4th test sample. In previous studies on the subject, it has been emphasized that the hardness decreases from the recast layer to the base material [34, 35]. This change in microhardness can be ascribed to the quenching and alloying effect due to high temperature gradient. As declared in literatures, the high electrical discharge energy transmitted to the machining zone makes the conditions favorable for the formation of microhardness, Fe and carbide compounds or phases on the machined surface [36, 37].

3.3 | Fatigue life

Stress-cycle number (S–N) diagrams were achieved by rotating bending fatigue tests on the samples in ASTM E-466 standards, which were formed by processing AISI L2 cold work tool steel according to different machining parameters with the electrical discharge turning method. Fatigue tests were performed by applying different stress values between 2/3 and 1/3 of 1158 MPa, which is the tensile strength of the base material. The S–N diagrams obtained for the test samples processed according to the Taguchi L_9 experimental design is shown, Figure 7.

Test sample 1 has the maximum fatigue strength, and sample 2 shows strength close to it, Figure 7. This can be attributed to the lower surface roughness criteria (R_z, S_m) of the mentioned samples. That is, the low surface roughness reduced the possibility of initiating a fatigue damage mechanism. At the same time, this result means

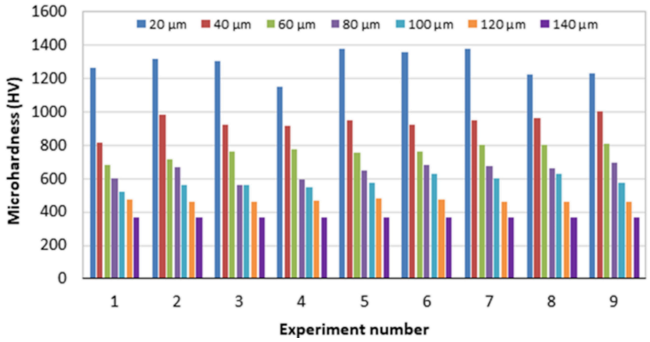

FIGURE 6 The microhardness variations of machined subsurfaces.

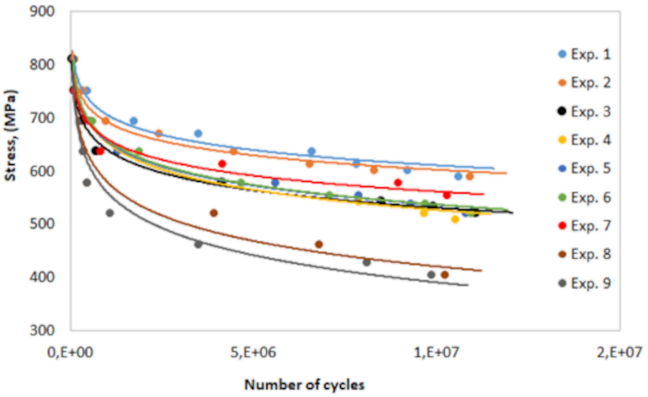

FIGURE 7 S–N diagrams for electrical discharge turning samples.

15214052, 2023, 1, Downloaded from https://onlinelibrary.wiley.com/doi/10.1002/mawe.202200119 by Gazi University, Wiley Online Library on [28/01/2023]. See the Terms and Conditions (https://onlinelibrary.wiley.com/terms-and-conditions) on Wiley Online Library for rules of use; OA articles are governed by the applicable Creative Commons License

that fatigue in the machine elements starts at higher stress values. Test sample 3 showed lower fatigue strength than test samples 1 and 2 processed at the same discharge current. This result was mainly due to the high roughness depending on the formation of deeper craters on the workpiece surface due to the high impact time applied in the sample 3 [38, 39]. High temperature during the electrical discharge machining process causes micro melting and vaporization of the material, creating pits, tears and peaks on the machined surface. These formations increase surface roughness, create local stress concentrations, and act as crack initiation, negatively affecting the fatigue behavior of the material [8, 21]. Alternatively, possible tensile residual stresses and increasing microhardness on the subsurface caused a decrease in the ductility of the material [11]. The fracture surface image of sample 3 supports these inferences, Figure 8. Brittle fracture event occurred in the sample 3, which has a deeper and wider crater surface, as a result of the cracks starting from the surface of the machined part getting bigger and deeper. As a result, the corresponding sample exhibited lower fatigue life due to rapid crack propagation.

Fatigue curves of samples 4–6 are similar and it is seen that they exhibit fatigue strengths close to each other. On the other hand, despite being processed at the highest current, sample 7 orders 3rd in terms of fatigue strength. This result can be attributed to the smooth surface morphology produced by using the smallest pulse duration and maximum pulse interval in the relevant experiment, Figure 4. In this sample, shallow craters formed on the surface and relatively low R_z value positively affected the fatigue strength. On the other hand, as seen from the fracture surface of sample 7, sudden fracture occurred due to high microhardness, Figure 9. From this, it turns out that the pulse duration or pulse interval is as effective as the discharge current on the fatigue strength of the parts processed by the electrical discharge machining. The smallest fatigue strength was obtained in sample 9, and this result was attributed to the highest level of surface quality criteria (R_z and S_m) formed as a result of machining with electrical discharge turning. As mentioned in research on the fatigue behavior of different materials by electrical discharge machining-processed, fatigue cracks progress either from surface craters or from pre-existing defects in the recast layer, such as microcracks and micro voids [9, 16, 18]. As a matter of fact, the deep surface craters and thick recast layer formed in this sample processed at the highest current and pulse duration support this result, Figure 10.

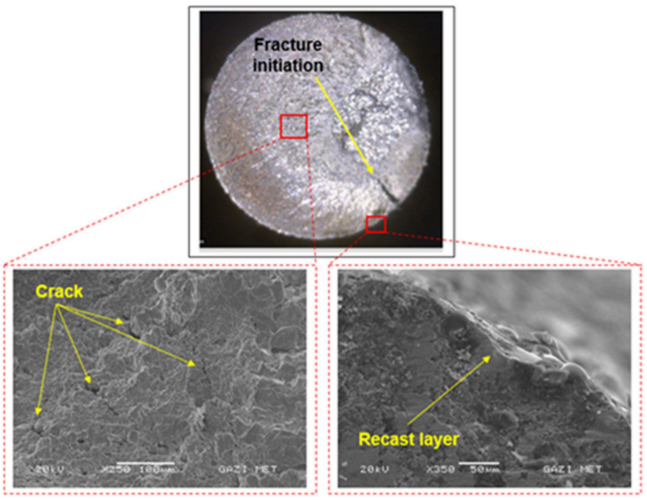

FIGURE 9 Scanning electron microscopy pictures of the fracture surface of sample 7.

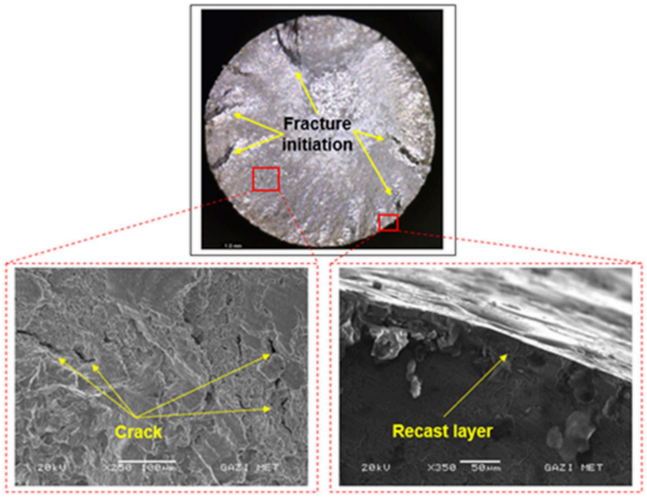

FIGURE 8 Scanning electron microscopy pictures of the fracture surface of sample 3.

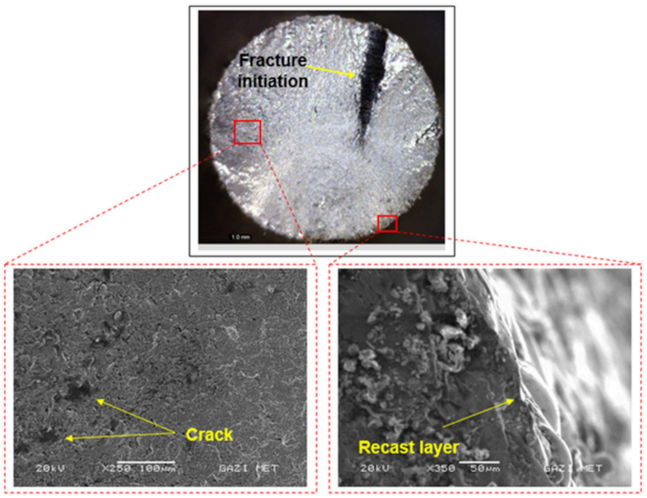

FIGURE 10 Scanning electron microscopy pictures of the fracture surface of sample 9.

15214052, 2023, 1, Downloaded from https://onlinelibrary.wiley.com/doi/10.1002/mawe.202200119 by Gazi University, Wiley Online Library on [28/01/2023]. See the Terms and Conditions (https://onlinelibrary.wiley.com/terms-and-conditions) on Wiley Online Library for rules of use; OA articles are governed by the applicable Creative Commons License

4 | CONCLUSIONS

This study presents detailed research on the surface quality, microhardness and fatigue behavior of parts produced from tool steel by electrical discharge turning using Taguchi experimental design. The results obtained are summarized below.

1. In electrical discharge turning turning, the pulse duration is more effective on the mean spacing of profile irregularities while the discharge current is more effective on the average surface roughness and maximum roughness depth. The lowest R_a, R_z and S_m values were obtained at discharge current of 3 A, pulse duration of 3 μs and pulse interval of 5 μs that is, these parameter levels are optimum in terms of surface quality.
2. Microhardness reached its highest levels in the high discharge current or medium discharge current-high impact interaction. It has been observed that the microhardness varies significantly up to a depth of 100 μm. The maximum microhardness was measured as 1376 HV in 20 μm depths from the machined sample with discharge current of 12 A, pulse duration of 3 μs and pulse interval of 7 μs.
3. Fatigue life was mostly affected by the R_z and S_m criteria, and it was determined that the fatigue life decreased as their values increased. As well, as a result of the fracture surface scanning electron microscopy investigations, brittle fractures occurred in some samples with relatively smooth surface topography. It was concluded that in such specimens, although shallow craters are formed, the high microhardness and thick recast layer cause sudden fractures, thus reducing the fatigue life. In this regard, it is recommended to machine the parts produced with electrical discharge machining technologies by using low pulse duration and discharge current and high pulse interval to achieve high fatigue life.
4. In the future, considering the mechanical properties and machining cost together in research on hybrid electrical discharge machining applications will make significant contributions to the relevant literature and sustainability.

ORCID

M. Günay http://orcid.org/0000-0002-1281-1359

REFERENCES

1. V. Gohil, Y. M. Puri, *Proc Inst Mech Eng B J Eng Manuf.* **2017**, *231*, 195.
2. E. Uhlmann, S. Piltz, S. Jerzembeck, *J. Mater. Process. Technol.* **2005**, *160*, 15.
3. I. S. Jawahir, E. Brinksmeier, R. M'Saoubi, D. K. Aspinwall, J. C. Outeiro, D. Meyer, D. Umbrello, A. D. Jayal, *CIRP Ann. - Manuf. Technol.* **2011**, *60*, 603.
4. H. Ramasawmy, L. Blunt, *J. Mater. Process. Technol.* **2004**, *148*, 155.
5. A. Monaca, J. W. Murray, Z. Liao, A. Speidel, J. A. Robles-Linares, D. A. Axinte, M. C. Hardy, A. T. Clare, *Int. J. Mach. Tools Manuf.* **2021**, *164*, 103718.
6. M. Zhang, Q. Zhang, L. Dou, Q. Liu, C. Dong, *J. Manuf. Process.* **2016**, *87*, 909.
7. H. B. Özerkan, *Mater. Today: Proc.* **2019**, *11*, 417.
8. A. Al-Khazraji, S. A. Amin, S. M. Ali, *Eng. Sci. Technol. Int J.* **2016**, *19*, 1400.
9. A. Pramanik, A. R. Dixit, S. Chattopadhyaya, M. S. Uddin, Y. Dong, A. K. Basak, G. Littlefair, *Adv. Manuf.* **2017**, *5*, 59.
10. A. Mohammadi, A. F. Tehrani, A. Abdullah, M. Danesh, *Proc Inst Mech Eng B J Eng Manuf.* **2014**, *228*, 1372.
11. R. B. Azhiri, A. S. Bideskan, F. Javidpour, R. M. Tekiyeh, *Int. J. Adv. Manuf. Technol.* **2019**, *101*, 2849.
12. M. Sarıkaya, V. Yılmaz, *Neural. Comput. Appl.* **2018**, *30*, 1503.
13. N. Kumar Chauhan, A. Kumar Das, S. Rajesha, *Mater. Today: Proc.* **2018**, *13*, 27178.
14. S. Ramesh, M. P. Jenarthanan, *Proc. Inst. Mech. Eng. E: J. Process Mech. Eng.* **2021**, *235*, 1092.
15. N. Faisal, K. Kumar, *Technologies.* **2018**, *6*, 54.
16. Z. Chen, J. Moverare, R. L. Peng, S. Johansson, *Procedia CIRP.* **2016**, *45*, 307.
17. A. Pramanik, A. K. Basak, *Int. J. Fatigue.* **2019**, *128*, 105186.
18. V. P. Srinivasan, P. K. Palani, *Ceram. Int.* **2020**, *46*, 10734.
19. P. Talebizadehsardari, A. Eyvazian, F. Musharavati, Q. Zeeshan, R. B. Mahani, T. A. Sebaey, *Int. J. Adv. Manuf. Technol.* **2021**, *112*, 719.
20. A. M. P. Jesus, G. F. S. Ramos, V. M. G. Gomes, M. J. Marques, M. A. V. Figueiredo, J. D. R. Marafona, *Int. J. Fatigue.* **2020**, *139*, 105742.
21. M. Lundberg, J. Saarimäki, J. J. Moverare, M. Calmunger, *Mater. Charact.* **2017**, *124*, 215.
22. M. Antar, P. Hayward, J. Dunleavey, P. Butler-Smith, *Procedia CIRP.* **2018**, *68*, 308.
23. J. E. A. Qudeiri, A. Zaiout, A. H. I. Mourad, M. H. Abidi, A. Elkaseer, *Appl. Sci.* **2020**, *10*, 2082.
24. R. Çakıroğlu, M. Günay, *J. Mater. Res. Technol.* **2020**, *9*, 7305.
25. K. H. Ho, S. T. Newman, *Int. J. Mach. Tools Manuf.* **2003**, *43*, 1287.
26. A. P. Dwivedi, S. K. Choudhury, *Mater. Manuf. Process.* **2016**, *31*, 1844.
27. J. E. A. Qudeiri, A. Saleh, A. Ziout, A. H. I. Mourad, M. H. Abidi, A. Elkaseer, *Materials.* **2019**, *12*, 907.
28. C. Cogun, Z. Esen, A. Genc, F. Cogun, N. Akturk, *Proc Inst Mech Eng B J Eng Manuf.* **2016**, *230*, 2190.
29. N. Ahmed, S. Anwar, K. Ishfaq, M. Rafaqat, M. Saleh, S. Ahmad, *Sci. Rep.* **2019**, *9*, 1.
30. Y. Murakami, *Metal Fatigue*, Elsevier Science Ltd, Oxford **2002**.
31. N. Sharma, G. Singh, M. Gupta, H. Hegab, M. Mia, *Mater. Res. Express.* **2019**, *6*, 096568.

15214052, 2023, 1, Downloaded from https://onlinelibrary.wiley.com/doi/10.1002/mawe.202200119 by Gazi University, Wiley Online Library on [28/01/2023]. See the Terms and Conditions (https://onlinelibrary.wiley.com/terms-and-conditions) on Wiley Online Library for rules of use; OA articles are governed by the applicable Creative Commons License

32. B. Ekmekci, O. Elkoca, A. E. Tekkaya, A. Erden, *Mach. Sci. Technol.* **2005**, *9*, 39.
33. Y. Yildiz, M. M. Sundaram, K. P. Rajurkar, A. Altintas, *Proc. Inst. Mech. Eng. E: J. Process Mech. Eng.* **2017**, *231*, 414.
34. H. Rahimi, S. Masoudi, M. Tolouei-Rad, *Int. J. Adv. Manuf. Technol.* **2022**, *118*, 1767.
35. A. S. Gill, S Kumar, *Arab. J. Sci. Eng.* **2018**, *43*, 1499.
36. O. Gülcan, İ. Uslan, Y. Usta, C. Çoğun, *Mach. Sci. Technol.* **2016**, *20*, 523.
37. M. Balanou, P. Karmiris-Obratański, B. Leszczyńska-Madej, E. L. Papazoglou, A. P. Markopoulos, *Machines.* **2021**, *9*, 268.
38. T. M. Mower, *Int. J. Fatigue.* **2014**, *64*, 84.
39. Z. Xu, J. Dunleavey, M. Antar, R. Hood, S. L. Soo, G. Kucukturk, C. J. Hyde, A. T. clare, *Int. J. Fatigue.* **2018**, *111*, 196.

How to cite this article: R. Çakıroğlu, M. Günay, *Materialwiss. Werkstofftech.* **2023**, *54*, e202200119. https://doi.org/10.1002/mawe.202200119

15214052, 2023, 1, Downloaded from https://onlinelibrary.wiley.com/doi/10.1002/mawe.202200119 by Gazi University, Wiley Online Library on [28/01/2023]. See the Terms and Conditions (https://onlinelibrary.wiley.com/terms-and-conditions) on Wiley Online Library for rules of use; OA articles are governed by the applicable Creative Commons License